

NASA Technical Memorandum 83353

# Aerodynamic-Wave Break-up of Liquid Sheets in Swirling Airflows and Combustor Modules

(NASA-TM-83353) AERODYNAMIC-WAVE BREAK-UP  
OF LIQUID SHEETS IN SWIRLING AIRFLOWS AND  
COMBUSTOR MODULES (NASA) 16 P HC AC2/HF A01  
CSCI 20D

N83-23545

Unclas

G3/34

03476

R. Ingebo  
*Lewis Research Center  
Cleveland, Ohio*



Prepared for the  
Nineteenth Joint Propulsion Conference and Technical Display  
cosponsored by the AIAA, SAE, and ASME  
Seattle, Washington, June 27-29, 1983

**NASA**

# AERODYNAMIC-WAVE BREAK-UP OF LIQUID SHEETS IN SWIRLING AIRFLOWS AND COMBUSTOR MODULES

R. Ingebo

National Aeronautics and Space Administration  
Lewis Research Center  
Cleveland, Ohio

## Abstract

Experimental mean drop diameter data were obtained for the atomization of liquid sheets injected axially downstream in high-velocity swirling and non-swirling airflow. Conventional simplex pressure-atomizing fuel nozzles and splash-type fuel injectors were studied under simulated combustor inlet airflow conditions. The following general empirical expression relating reciprocal mean drop diameter,  $D_m^{-1}$ , to airstream mass velocity,  $\rho_a V_a$ , was obtained:  $D_m^{-1} = D_{m,i}^{-1} + C[(\rho_a V_a - (\rho_a V_a)_i)]$ , where  $(\rho_a V_a)_i$  is the value of  $\rho_a V_a$  at which aerodynamic-wave break-up of liquid sheets occurs.  $D_{m,i}^{-1}$  is the value of  $D_m^{-1}$  when  $\rho_a V_a = (\rho_a V_a)_i = 10 \text{ g/cm}^2\text{-sec}$  that was used in comparing atomization results obtained with different types of fuel injectors. The finest degree of atomization, i.e. the highest value of the coefficient  $C$ , was obtained with swirl can combustor modules ( $C = 15$ ) as compared with pressure-atomizing nozzles ( $C = 12$ ).

## Nomenclature

$C$	coefficient for aerodynamic-wave break-up of liquid sheets and jets
$D_m^{-1}$	diameter, cm reciprocal mean drop diameter, $\sum n D_d^{-2} / \sum n D_d^3, \text{ cm}^{-1}$
$n$	number of drops in given size range
$Re$	Reynolds number, $\rho V D / \mu$
$V$	velocity, cm/sec
$\mu$	dynamic viscosity, g/cm-sec
$\rho$	density, g/cm <sup>3</sup>

## Subscripts:

$a$	airstream
$d$	droplet
$i$	initial
$l$	liquid
$o$	orifice

## Introduction

The performance of liquid-fueled gas turbine combustors is markedly affected by the type of fuel injector selected to atomize the fuel. This has been demonstrated by combustor performance and exhaust emission data obtained in Refs. 1 and 2. Up to the present time, liquid atomization data have been lacking that can be used to specifically relate engine performance and emissions to the effect of swirling airflow on fuel atomization in a combustor primary-zone. Since airswirlers give improved mixing of fuel and air in the combustor primary-zone, they are extensively used in advanced combustor studies such as those described in Refs. 3 and 4. In Ref. 3, four different types of airswirlers with various blade angles and configurations were tested and good results were obtained with a 70° blade-angle axial airflow swirler. In Ref. 4, it was found that exhaust pollutants can be reduced considerably by using

the aerodynamic force of swirling airflows to atomize liquid fuel sheets or films instead of relying on the hydrodynamic pressure drop of the fuel as the energy source which is so commonly used in pressure atomizing simplex fuel nozzles. Thus, the reduction in pollutants was attributed to improved fuel atomization. In a more recent study, nitrogen oxide emissions in the exhaust gases of swirl can combustor modules were found to vary directly with the square of the mean drop diameter of the fuel spray as reported in Ref. 5.

Numerous investigations have been made regarding the atomization of liquid sheets, especially those produced in quiescent air with simplex pressure atomizing fuel nozzles i.e. Ref. 6. In Ref. 7, a comparison was made of mean drop sizes produced by various types of liquid sheet break-up in axial non-swirling airflows. It was found that splash-plate fuel injectors which are now used in swirl-can combustor modules produced sprays with improved fineness of atomization, i.e. higher reciprocal mean drop diameter,  $D_m^{-1}$ , values than the simplex nozzle when the weight flow rate per unit area or mass velocity of the airstream,  $\rho_a V_a$ , exceeded  $10 \text{ g/cm}^2\text{-sec}$  i.e. when aerodynamic-wave break-up occurred. However, at low mass velocities the simplex pressure atomizing nozzle gave higher values of  $D_m^{-1}$  than the splash-plate fuel injector. Atomization data were also obtained for the break-up of liquid sheets produced with impinging jet fuel injectors used in rocket combustors. However, the study was limited to liquid sheet break-up in axial non-swirling airflows.

In the present investigation, experiments were conducted in which combustor inlet airflow conditions were simulated to determine the effect of mass velocity,  $\rho_a V_a$ , of non-swirling and swirling airflow on the atomization of liquid sheets produced with conventional simplex pressure atomizing fuel nozzles and splash type fuel injectors. A 70° blade-angle airswirler and a pair of concentric contra-rotating air-swirlers were used to produce swirling airflows. The effect of aerodynamic force on mean drop diameter was studied primarily in the aerodynamic-wave break-up regime. In Ref. 8, it was found that capillary-wave break-up occurs when hydrodynamic and aerodynamic forces are relatively low and aerodynamic-wave (or acceleration-wave) break-up occurs when air velocity is high relative to liquid velocity. In this study, aerodynamic-wave break-up is emphasized because of the increasingly higher airflow requirements of advanced high pressure and high temperature gas turbine combustors. Previous studies of capillary-wave and acceleration-wave break-up of both liquid jets and sheets are discussed in the Appendix.

Non-swirling and swirling liquid sheets were injected into non-swirling and swirling airflows. Mean drop diameter data were obtained from water sprays produced by air atomizing splash plate and conventional simplex pressure atomizing fuel nozzles. Non-swirling liquid sheets produced by splash plates were injected radially in airstreams and swirling hollow-cone sheets produced by

simplex nozzles were injected at cone-angles of 45° and 80°, respectively, in non-swirling and swirling airflows in a 7.6 cm inside diameter duct. Airstream mass velocity,  $\rho_a V_a$ , was varied from 1.5 to 25.7 g/cm<sup>2</sup>-sec at an air temperature of 293 K and atmospheric pressure at the duct exit. Orifice diameters varied from 0.090 to 0.340 cm and 0.051 to 0.46 cm for simplex and splash plate fuel injectors, respectively. Thus, under simulated combustor conditions, mean drop diameter data were obtained and correlated with aerodynamic force based on airstream mass velocity,  $\rho_a V_a$ .

#### Apparatus and Procedure

Fuel injectors were mounted in the open-duct facility as shown in Fig. 1. Airflow was drawn from the laboratory supply system, at ambient temperature (283 K) and exhausted into the atmosphere. The airflow control valve was opened until the desired airflow rate per unit area was obtained. The bellmouth test section shown in Fig. 1 has a total length of 0.152 m, an inside diameter of 0.096 m and is mounted inside of a duct that is 5 m in length with an inside diameter of 0.152 m.

Water sheets were produced at the duct center line and directed axially downstream with the fuel injectors shown in Figs. 2 to 4. The water flow rate was controlled, by gradually opening and regulating the valve, over a range of 27 to 68 liter/hour. A single 70° blade-angle airswirler and one of the simplex pressure-atomizing fuel nozzles is shown in Fig. 2. Two different simplex fuel nozzles were tested which produced 45° cone-angle sprays, namely nozzles Nos. 1 and 2 with orifice diameters of 0.09 and 0.13 cm, respectively. Also, two simplex nozzles that produce 80° cone-angle sprays were used, namely nozzles Nos. 3 and 4 having orifice diameters of 0.23 and 0.34 cm, respectively. Fuel nozzle characteristics are given in Table I.

Three types of splash plate fuel injectors that were investigated are shown in Figs. 3(a) to (c). Two different fuel tubes having orifice diameters of 0.1016 and 0.216 cm, respectively, were used with the splash-disk fuel injector shown in Fig. 3(a). The splash-cone fuel injector, shown in Fig. 3(b), has four 0.157 cm-diameter orifices equally spaced around the circumference of the fuel tube. The splash-groove fuel injector, shown in Fig. 3(c), has three 0.051 cm-diameter orifices equally spaced in the small groove and six 0.051 cm-diameter orifices in the large groove.

Four swirl-can combustor modules were studied that had been used in a previous combustor study as described in Ref. 5 and diagrams of the modules are shown in Fig. 4. Each module consists primarily of a dual concentric contra-rotating airswirler configuration with a splash disk type fuel injector. Further details of module construction are given in Ref. 5.

After water and airflow rates were set, mean drop diameter data were obtained with the scanning radiometer mounted 11.4 cm downstream of the open-duct exit. The scanning radiometer optical system shown in Fig. 5 consisted of a 1-milliwatt helium-neon laser, a 0.003 cm-diameter aperture, a 7.5 cm-diameter collimating lens, a 10 cm-diameter converging lens, a 5 cm-diameter collecting lens, a scanning disk with a 0.05 by 0.05 cm slit, a timing light, and a photomultiplier detector. A more complete description of the scanning

radiometer, the mean drop diameter range, and the method of determining mean particle size are discussed in Refs. 9 and 10.

#### Experimental Results

The aerodynamic-wave break-up of liquid sheets in non-swirling and swirling airflow was investigated in a simulated gas turbine combustor primary-zone. Mean drop diameter data were obtained for water sheets atomized under simulated combustor inlet airflow conditions. Swirling hollow-cone sheets of water were injected axially downstream with pressure-atomizing simplex fuel nozzles in the first portion of the investigation. Then, radially injected sheets produced with splash plate fuel injectors and finally swirl-can combustor modules were investigated. Airflow test conditions are given in Table II and show the variation of inlet-air static pressure with airflow mass velocity, with and without the use of an airswirler.

#### Pressure-Atomizing Simplex Fuel Nozzles

Mean drop diameters were determined for the break-up of swirling hollow-cone water sheets injected axially downstream in swirling and non-swirling airflow. For swirling airflow, the simplex fuel nozzle No. 1 shown in Fig. 2 was used with an attached airswirler. As a measure of fineness of atomization or spray specific-surface area, the reciprocal mean drop diameter,  $D_m^{-1}$ , was determined with the scanning radiometer and plotted against mass velocity,  $\rho_a V_a$ , as shown in Fig. 6. Mean drop diameter data obtained with the same fuel nozzle No. 1 used in Ref. 7 for the case of non-swirling airflow, is also shown in Fig. 6 for comparison. From this plot it is evident that with low airflow rate per unit area, i.e.  $\rho_a V_a < 7$ , the values of  $D_m^{-1}$  are quite similar for swirling and non-swirling airflow. This is attributed to hydrodynamic forces controlling atomization which occurs primarily in the capillary-wave break-up regime. A discussion of previous studies of capillary-wave and aerodynamic-wave break-up of liquid jets and sheets is given in the Appendix.

When  $\rho_a V_a$  exceeds 10 g/cm<sup>2</sup>-sec with swirling airflow or 15 g/cm<sup>2</sup>-sec with non-swirling airflow, then aerodynamic-wave break-up appears to control the atomization process and specific-surface area in terms of  $D_m^{-1}$  increases rapidly as  $\rho_a V_a$  increases. A similar effect of  $\rho_a V_a$  on  $D_m^{-1}$  was obtained at relatively low values of  $\rho_a V_a$  with water sprays produced by a pressure-atomizing simplex fuel nozzle and analyzed with a "Malvern" light scattering instrument in Ref. 11. The fuel nozzle used in that study had the same 45° cone-angle but a different flow number from that of fuel nozzle No. 1.

From Fig. 6, the following general relationship is obtained for aerodynamic-wave break-up of a swirling hollow-cone sheet of liquid in both swirling and non-swirling airflow:

$$D_m^{-1} = D_{m,i}^{-1} + 12[\rho_a V_a - (\rho_a V_a)_i] \quad (1)$$

A similar expression was derived in Ref. 7 for non-swirling airflow. For fuel nozzle No. 1, the expression may be rewritten for non-swirling airflow as,  $D_m^{-1} = 220 + 12(\rho_a V_a - 15)$  and for swirling airflow,  $D_m^{-1} = 245 + 12(\rho_a V_a - 10)$ . Comparison of these two expressions shows that swirling airflow is considerably more effective

than non-swirling airflow in producing a spray of relatively high  $D_m^{-1}$  or specific-surface area. Improvement with the airswirler is attributed to an observed twisting and stretching out of the swirling liquid sheet when it is in contract with a rotating vortex airflow produced by the 70° blade-angle airswirler. Shear force due to velocity gradients produced by deflection and acceleration of the airflow appeared to increase the rate of momentum transfer to the liquid sheet and thereby increase the reciprocal mean drop diameter,  $D_m^{-1}$ , or spray specific-surface area.

The general relationship, Eq. (1), may be rewritten in nondimensional form for aerodynamic-wave break-up of liquid sheets in terms of the airflow Reynolds number,  $Re_a$ , as follows:

$$\frac{D_o}{D_{m,i}} = \frac{D_a}{D_{m,i}} + 2.2 \times 10^{-3} (Re_a - Re_{a,i}) \quad (2)$$

where  $\mu_a = 1.81 \times 10^{-4}$  g/cm-sec and  $Re_{a,i}$  is the airflow Reynolds number at which aerodynamic-wave break-up appears to be initiated.

Variations of reciprocal mean drop diameter  $D_m^{-1}$ , with airflow mass velocity,  $\rho_a V_a$ , are shown in Fig. 7 for fuel nozzle No. 2 which has a somewhat larger orifice diameter and flow number than fuel nozzle No. 1, as shown in Table I. Initially in quiescent air,  $\rho_a V_a = 0$ , values of  $D_m^{-1}$  are somewhat lower for nozzle No. 2 as expected since the data were obtained with a liquid flow rate of 68 liters/hr as compared with only 27.2 liters per hour flow for nozzle No. 1. This comparison is shown in Table III. For the case of non-swirling airflow and  $\rho_a V_a = 10$ , the value of  $D_m^{-1}$  was less for nozzle No. 2 than for the smaller nozzle No. 1. However, with swirling airflow the larger nozzle No. 2 gave a value of  $D_m^{-1}$  approximately 20 percent higher than that obtained for nozzle No. 1. This improvement in fineness of atomization in swirling airflow, with the larger nozzle No. 2, is attributed to improved penetration of a high momentum liquid sheet into the airflow using a larger orifice diameter and a higher liquid flow rate. The transition from capillary to acceleration wave break-up was marked by a large increase in  $D_m^{-1}$  with nozzles No. 2.

The general Eq. (1) may be rewritten for nozzle No. 2 and non-swirling airflow as follows:  $D_m^{-1} = 145 + 12 (\rho_a V_a - 10)$  and for swirling airflow:  $D_m^{-1} = 290 + 12 (\rho_a V_a - 10)$ . Thus, as shown in Table III, the value of  $D_m^{-1}$  for nozzle No. 1 at  $\rho_a V_a = 10$  was increased approximately 100 percent by using the 70° blade-angle airswirler to produce swirling airflow and break-up the liquid sheet.

Figures 8 and 9 show the effect of airflow mass velocity,  $\rho_a V_a$ , on reciprocal mean drop diameter,  $D_m^{-1}$ , of sprays produced with fuel nozzles No. 3 and 4 having orifice diameters of 0.23 and 0.34 centimeter, respectively. Both nozzles produced 80° cone-angle sprays at a water flow rate of 68 liter per hour. As shown in Fig. 8 and Table III, only a small increase of approximately 10 percent in  $D_m^{-1}$  or fineness of atomization was obtained with nozzle No. 3 having a cone-angle of 80° as compared with the 45° cone-angle nozzle No. 2.

Fuel nozzle No. 4 has the largest orifice diameter of all of the pressure atomizing fuel nozzles used in this study. As shown in Fig. 9 and Table III, it gave values of  $D_m^{-1}$  slightly less than those obtained with nozzle No. 3. This was attributed to the lower turbulence level of

the liquid sheet which was produced at a considerably lower liquid velocity with the 0.34 centimeter diameter orifice than with the 0.23 centimeter diameter orifice. Mean drop size data for  $\rho_a V_a < 7$  were not obtained since such data would fall below the aerodynamic-break-up regime.

Equation (1) may be rewritten for nozzle No. 3 as:  $D_m^{-1} = 160 + 12 (\rho_a V_a - 10)$  and  $D_m^{-1} = 320 + 12 (\rho_a V_a - 10)$  for non-swirling and swirling airflow, respectively. Nozzle No. 4 gave similar expressions i.e.  $D_m^{-1} = 150 + 12 (\rho_a V_a - 10)$  and  $D_m^{-1} = 310 + 12 (\rho_a V_a - 10)$  for non-swirling and swirling airflow respectively. Like fuel nozzle No. 2, fuel nozzles No. 3 and 4 both gave increases of approximately 100 percent in the value of  $D_m^{-1}$  or specific-surface area, by using an airswirler to improve liquid sheet break-up.

### Splash Plate Fuel Injectors

Water sheets were injected radially in non-swirling and swirling airflows with three different splash-type fuel injectors. The splash-disk fuel injector shown in Fig. 3(b) gave a variation of reciprocal mean drop diameter with airstream mass velocity as shown in Fig. 10, using orifice diameters of 0.1016 and 0.216 centimeters. Thus for splash plate injectors and swirling airflow, the general expression is obtained

$$D_m^{-1} = D_{m,i}^{-1} + 13 [\rho_a V_a - (\rho_a V_a)_i] \quad (3)$$

Thus, at  $\rho_a V_a = 10$ :  $D_m^{-1} = 355$  and  $335 \text{ cm}^{-1}$  when  $D_o = 0.1016$  and  $0.216 \text{ cm}$ , respectively. This expression agrees well with the relation  $D_m^{-1} = 355 + 13 \rho_a V_a$  which was obtained in Ref. 7 for non-swirling airflow, and  $D_o = 0.1016 \text{ cm}$ .

The effect of the airswirler on liquid sheet break-up as shown in Fig. 10 is similar to but somewhat more pronounced than that observed with simplex fuel nozzles. This may be attributed to the fact that the airflow angle of attack relative to the liquid sheet is 90° as compared with the simplex nozzles having cone angles of either 45° or 80°, i.e. angles of attack of 22.5° and 40°, respectively.

Similar experiments were conducted with splash-cone and splash-groove fuel injectors shown in Figs. 3(b) and (c). As shown in Fig. 11, a marked increase in reciprocal mean drop diameter,  $D_m^{-1} = 345 + 13 (\rho_a V_a - 10)$  for the splash-groove fuel injector and  $D_m^{-1} = 325 + 13 (\rho_a V_a - 10)$  for the splash-cone fuel injector. The slightly lower value of  $D_m^{-1}$  for the splash-cone fuel injector is attributed to the use of a relatively large orifice diameter of 0.157 cm as compared with the splash-groove orifice diameter of 0.051 cm.

Values of  $D_m^{-1}$  obtained with the three splash type fuel injectors were considerably higher than those obtained using the simplex pressure-atomizing fuel nozzles at relatively high values of airflow mass velocity,  $\rho_a V_a$ . However, at low airflow rates the simplex fuel nozzles gave somewhat higher values of  $D_m^{-1}$  since they were designed to more efficiently use the hydrodynamic force in breaking-up the liquid sheet. In terms of airflow Reynolds number, Eq. (2) may be rewritten to give the following general relationship:

$$D_o/D_m = D_o/D_{m,i} + 2.4 \times 10^{-3} (Re_a - Re_{a,i}) \quad (4)$$

for acceleration-wave break-up of liquid sheets injected in swirling airflows with splash-type fuel injectors.

#### Swirl-Can Combustor Modules

Fuel injector used in swirl-can combustor modules are generally the splash-plate type of atomizer. It is similar to the splash-disk fuel injector used in the present study. However, as shown in Fig. 4, a pair of concentric contra-rotating airswirlers are used to enhance fuel-air mixing and burning instead of the conventional single airswirler. Values of the reciprocal mean drop diameter are plotted as a function of mass velocity in Fig. 12 and give the following relationship:

$$D_m^{-1} = D_{m,i}^{-1} + 15[\rho_a V_a - (\rho_a V_a)_i] \quad (5)$$

which shows some improvement in fineness of atomization when a dual concentric contra-rotating airswirler is used as compared with Eq. (3) for the splash-plate fuel injector used with a conventional single airswirler. In the case of swirl-can No. 8, Fig. 12 shows that  $D_{m,i}^{-1} = 390$  at  $(\rho_a V_a)_i = 10$ . With this injector, the liquid fuel is injected upstream on the hub of the inner airswirler. For swirl-can No. 9, water is injected downstream of the inner airswirler which is also recessed within the outer airswirler. In this case, the value of  $D_{m,i}^{-1}$  is considerably higher, i.e.  $D_{m,i}^{-1} = 430$ . Swirl-can No. 10 has an inner airswirler flush with the outer airswirler and water is again injected downstream of the airswirler with a splash-plate fuel injector. Here the value of  $D_{m,i}^{-1}$  is only  $370 \text{ cm}^{-1}$  which indicates that a recessed inner airswirler like that used for swirl-can No. 9 is beneficial in giving higher values of  $D_m^{-1}$  for high specific-surface area sprays. It is also interesting to note here that in Ref. 5, swirl-can No. 9 also gave the best atomization results.

To determine the effect of orifice diameter on  $D_m^{-1}$  two different orifice diameters of 0.081 and 0.46 cm, respectively, were used with the swirl-can combustor module previously used in Ref. 12. As shown in Fig. 12, the smaller orifice diameter 0.081 cm, gave a considerably higher value of  $D_m^{-1}$  than the larger orifice diameter of 0.46 cm, i.e.  $D_{m,i}^{-1} = 345$  and  $294 \text{ cm}^{-1}$ , respectively. In terms of airflow Reynolds number, Eq. (2) may be rewritten to give the following general relationship:

$$D_o/D_m = D_o/D_{m,i} + 2.7 \times 10^{-3} (Re_a - Re_{a,i}) \quad (6)$$

for acceleration-wave break-up of liquid sheets produced in swirl-can combustor modules. The coefficient  $2.7 \times 10^{-3}$  is approximately 23 percent higher than that obtained for pressure-atomizing fuel nozzles as given in Eq. (2) and indicates an improvement in fineness of atomization.

#### Summary of Results

Empirical correlations of reciprocal mean drop diameter with airflow mass velocity were derived for aerodynamic-wave break-up of liquid sheets in non-swirling and swirling airflows. A scanning radiometer gave mean dropsize data over an airflow mass velocity range of 1.5 to  $25.7 \text{ g/cm}^2\text{-sec}$ . Single and multiple airswirlers

were used to break-up liquid sheets produced by simplex pressure-atomizing nozzles and air-atomizing splash type fuel injectors and gave the following experimental results:

1. Each fuel injector gave mean drop size data for aerodynamic break-up of liquid sheets that could be correlated with airflow mass velocity according to the empirical relationship,

$$D_m^{-1} = D_{m,i}^{-1} + C[\rho_a V_a - (\rho_a V_a)_i]$$

where  $D_{m,i}^{-1}$  is the reciprocal mean drop diameter evaluated at  $(\rho_a V_a)_i$ , i.e. the airflow mass velocity at which aerodynamic-wave break-up appears to be initiated. This relation may also be expressed non-dimensionally as:

$$\frac{D_o}{D_m} = \frac{D_o}{D_{m,i}} + \mu C(Re_a - Re_{a,i})$$

2. Simplex fuel nozzles and splash plate fuel injector used with a single airswirler gave values of the coefficient for acceleration-wave break-up,  $C$ , of 12 and 13, respectively, whereas swirl can combustor modules with a dual airswirler and a splash plate fuel injector gave a value of  $C = 15$ . Improved fineness of atomization is indicated by a higher value of  $C$ .

3. At an airflow mass velocity of  $\rho_a V_a = 15 \text{ g/cm}^2\text{-sec}$ , the relatively small simplex nozzle No. 1 ( $D_o = 0.09 \text{ cm}$ ) gave a 40 percent increase in spray surface area as  $D_m^{-1}$  increased from 220 to  $310 \text{ cm}^{-1}$  whereas the largest simplex nozzle No. 4 ( $D_o = 0.34 \text{ cm}$ ) gave an increase of approximately 75 percent in  $D_m^{-1}$  which increased from 210 to  $370 \text{ cm}^{-1}$  with the use of a single airswirler.

4. At an airflow mass velocity of  $15 \text{ g/cm}^2\text{-sec}$  and with the use of a single airswirler, values of  $D_m^{-1}$  were 385, 405, and  $420 \text{ cm}^{-1}$  for cone, groove and disk types of splash plate fuel injectors, respectively. As indicated by the highest value of  $D_m^{-1}$ , the disk type with  $D_o = 0.102 \text{ cm}$  gave the finest atomization for a splash-type injector.

5. Swirl can combustor module No. 9 with a dual concentric airswirler and an airflow mass velocity of  $15 \text{ g/cm}^2\text{-sec}$  gave a value of  $D_m^{-1}$   $510 \text{ cm}^{-1}$  that was considerably above  $D_m^{-1}$  values of 470 and  $450 \text{ cm}^{-1}$  obtained for module No. 8 and 10, respectively. Of all the types of fuel injectors investigated, swirl can combustor module No. 9 gave the highest value of  $D_m^{-1}$  when  $\rho_a V_a > 10 \text{ g/cm}^2\text{-sec}$ . However, as expected the beneficial effect of single or multiple airswirlers on liquid sheet break-up is decreased markedly when mass velocity is reduced below  $10 \text{ g/cm}^2\text{-sec}$ .

6. The use of an airswirler improved atomization by producing higher values of reciprocal mean drop diameter,  $D_m^{-1}$ , than could be produced in non-swirling airstream having the same mass velocity,  $\rho_a V_a$ .

#### Appendix

##### Liquid Jet and Sheet Atomization in Non-Swirling Airflow

In two previous studies, Refs. 7 and 13, it was found that two general types of liquid atomization occur when a liquid jet or sheet breaks up in an airstream. Capillary-wave break-up occurs if the aerodynamic force of the airstream is relatively low. In this case, hydrodynamic force may

control the break-up process. However, when aerodynamic force is relatively large, atomization occurs in the aerodynamic-wave regime.

#### Capillary-Wave Atomization of Liquid Jets

In a previous experimental investigation, described in Ref. 13, the break-up of liquid jets injected normal to the airflow was studied and the variation of mass velocity,  $\rho_a V_a$ , with reciprocal mean drop diameter,  $D_m^{-1}$ , was determined as shown in Fig. 13. From this figure, the following expressions are obtained from capillary-wave break-up:

$$D_m^{-1} = 35.5(\rho_a V_a)^{0.75}$$

for  $\rho_a V_a < 10$  and an orifice diameter,  $D_o$ , of 0.033 cm, and:

$$D_m^{-1} = 18(\rho_a V_a)^{0.75}$$

for  $\rho_a V_a < 4$  and an orifice diameter of 0.132 cm.

#### Aerodynamic-Wave Atomization of Liquid Jets

From Fig. 13, the following expressions are obtained for aerodynamic-wave break-up of a liquid jet:

$$D_m^{-1} = 200 + 12.6[(\rho_a V_a - (\rho_a V_a)_i)]^{1.2}$$

for  $\rho_a V_a > 10$  and  $D_o = 0.033$  cm, and:

$$D_m^{-1} = 52 + 9.8[(\rho_a V_a - (\rho_a V_a)_i)]^{1.2}$$

for  $\rho_a V_a > 4$  and  $D_o = 0.132$  cm, and:

#### Aerodynamic-Wave Atomization of Swirling-Liquid Sheets

In a previous experimental study described in Ref. 7, the break-up of a swirling liquid sheet produced in non-swirling airflow with simplex pressure atomizing nozzles gave the variation of  $D_m^{-1}$  with  $\rho_a V_a$  as shown in Fig. 14. Downstream injection in non-swirling axial airflow gave the following expression for aerodynamic wave break-up:

$$D_m^{-1} = 220 + 12[(\rho_a V_a - (\rho_a V_a)_i)]$$

for  $\rho_a V_a > 15$  i.e.  $(\rho_a V_a)_i = 15$ , and  $D_o = 0.090$  cm, and:

$$D_m^{-1} = 145 + 12[(\rho_a V_a - (\rho_a V_a)_i)]$$

for  $\rho_a V_a > 10$  i.e.  $(\rho_a V_a)_i = 10$ , and  $D_o = 0.130$  cm. Thus, the general expression may be written as:

$$D_m^{-1} = D_{m,i}^{-1} + 12[(\rho_a V_a - (\rho_a V_a)_i)]$$

for aerodynamic-wave break-up in non-swirling airflow.

#### References

1. Mularz, E. J., Wear, J. D., and Verbulecz, P. W., "Pollution Emissions from Single Swirl-Can Combustor Modules at Parametric Test Conditions," NASA TM X-3167, 1975.
2. Norgren, C. T., and Riddlebaugh, S. M., "Effect of Fuel Injector Type on Performance and Emissions of Reverse-Flow Combustor," NASA TP-1945, 1981.
3. Ingebo, R. D., Daskocil, A. J. and Norgren, C. T., "High-Pressure Performance of Combustor Segments Utilizing Pressure-Atomizing Fuel Nozzles and Airswirlers for Primary-Zone Mixing," NASA TN D-6491, 1971.
4. Ingebo, R. D., and Norgren, C. T., "High-Pressure Combustor Exhaust Emissions with Improved Air-Atomizing and Conventional Pressure-Atomizing Fuel Nozzles," NASA TN D-7154, 1973.
5. Ingebo, R. D., "Atomizing Characteristics of Swirl-Can Combustor Modules with Swirl Blast Fuel Injectors," NASA TM-79297, 1980.
6. Simmons, H. C., "The Prediction of Sauter Mean Diameter for Gas Turbine Fuel Nozzles of Different Types," ASME Paper 79-WA/GT-5, Dec. 1979.
7. Ingebo, R. D., "Hydrodynamic and Aerodynamic Break-up of Liquid Sheets," NASA TM-82800, 1982.
8. Adelberg, M., "Mean Drop Size Resulting from the Injection of a Liquid Jet into a High-Speed Gas Stream," AIAA Journal, Vol. 6, No. 6, June 1968, pp. 1143-1147.
9. Buchele, D. R., "Scanning Radiometer for Measurement of Forward-Scattered Light to Determine the Mean Diameter of Spray Particles," NASA TM X-3454, 1976.
10. Ingebo, R. D., "Effect of Airstream Velocity on mean Drop Diameter of Water Sprays Produced by Pressure and Air Atomizing Nozzles," NASA TM-73740, 1977.
11. Johnson, S. M., "Venturi Nozzle Effects on Fuel Drop Size and Nitrogen Oxide Emissions," NASA TP-2028, 1982.
12. Wear, J. D., Trout, A. M. and Smith, J. M., "Low-Pressure Performance of Annular, High-Pressure (40-atm.), High Temperature (2480 K) Combustion System," NASA TP-1713, 1980.
13. Ingebo, R. D., "Capillary and Acceleration Wave Break-up of Liquid Jets in Axial-Flow Airstreams," NASA TP-1791, 1981.

TABLE I. - SIMPLEX FUEL NOZZLE CHARACTERISTICS

Fuel nozzle designation	Orifice diameter, $D_o$ , cm	Flow number $L/hr (N/M^2)^{0.5}$	Spray angle, deg
1	0.090	0.014	45
2	.130	.034	45
3	.230	.091	80
4	.340	.301	80

ORIGINAL PAGE IS  
OF POOR QUALITY

TABLE II. - AIRFLOW TEST CONDITIONS

Mass velocity, $\rho_a V_a$ , g/cm <sup>2</sup> -sec	Inlet-air static pressure	
	Without air swirler, kPa	With single airswirler, kPa
7.3	0.108	0.115
11.0	.112	.139
14.7	.117	.167
18.3	.124	.198
22.0	.132	----
25.7	.143	----

TABLE III. - EXPERIMENTAL CONSTANTS FOR AERODYNAMIC-WAVE BREAK-UP

EXPRESSION:  $D_m^{-1} = D_{m,i}^{-1} + C[\rho_a V_a - (\rho_a V_a)_i]$

Fuel injector	$D_o$ , cm	C	$D_{m,i}^{-1}$ , cm, evaluated at $(\rho_a V_a)_i = 10$ g/cm <sup>2</sup> -sec		
			Non-swirling airflow	With single air swirler	With double air swirler
Nozzle No. 1	0.090	12	170	245	---
Nozzle No. 2	.130	↓	145	290	---
Nozzle No. 3	.230		160	320	---
Nozzle No. 4	.340		150	320	---
Splash-disk	0.0102	13	200	355	---
Splash-disk	.216	↓	145	335	---
Splash-cone	.157		---	325	---
Splash-groove	.015		140	345	---
Swirl Can No. 9	0.130	15	---	---	430
Swirl Can No. 8	.130	↓	---	---	390
Swirl Can No. 10	.130		---	---	370
Swirl Can Used in Ref. 12	.081		---	---	345
Swirl Can Used in Ref. 12	.460		---	---	295

ORIGINAL PAGE IS  
OF POOR QUALITY

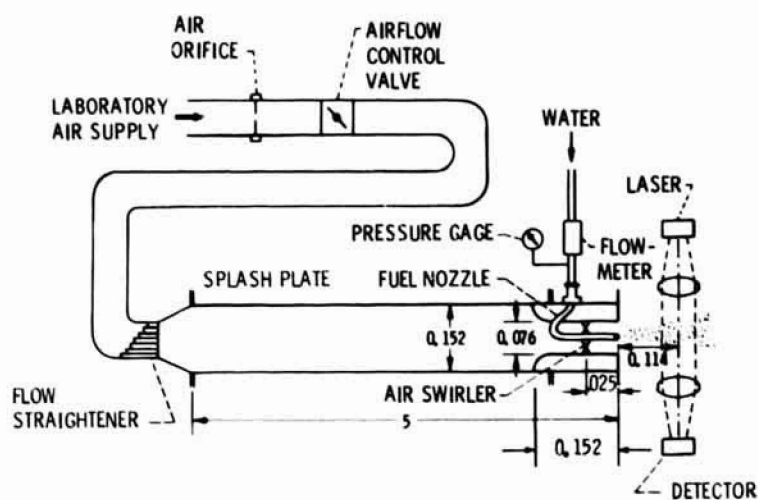
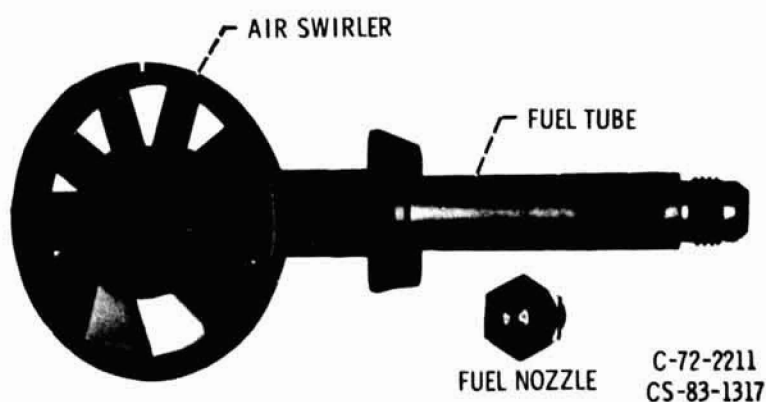


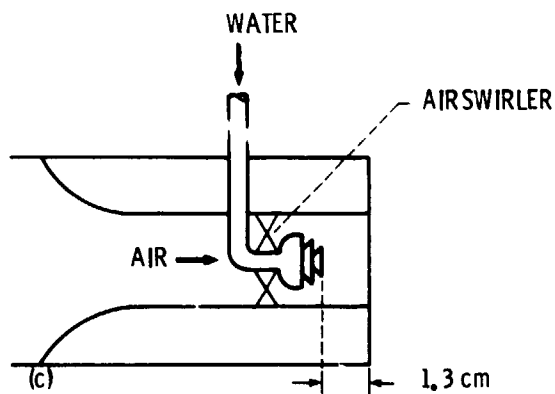
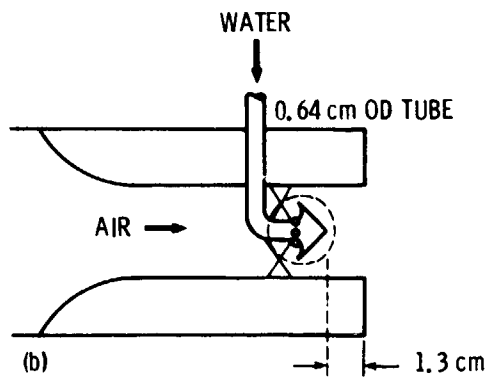
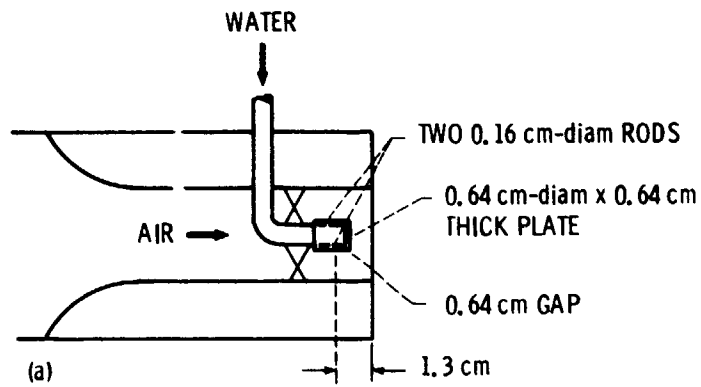
Figure 1. - Test facility and auxiliary equipment. (Dimensions are in meters.)



FUEL NOZZLE, AIR SWIRLER, AND FUEL TUBE.

Figure 2. - Simplex pressure-atomizing nozzles.

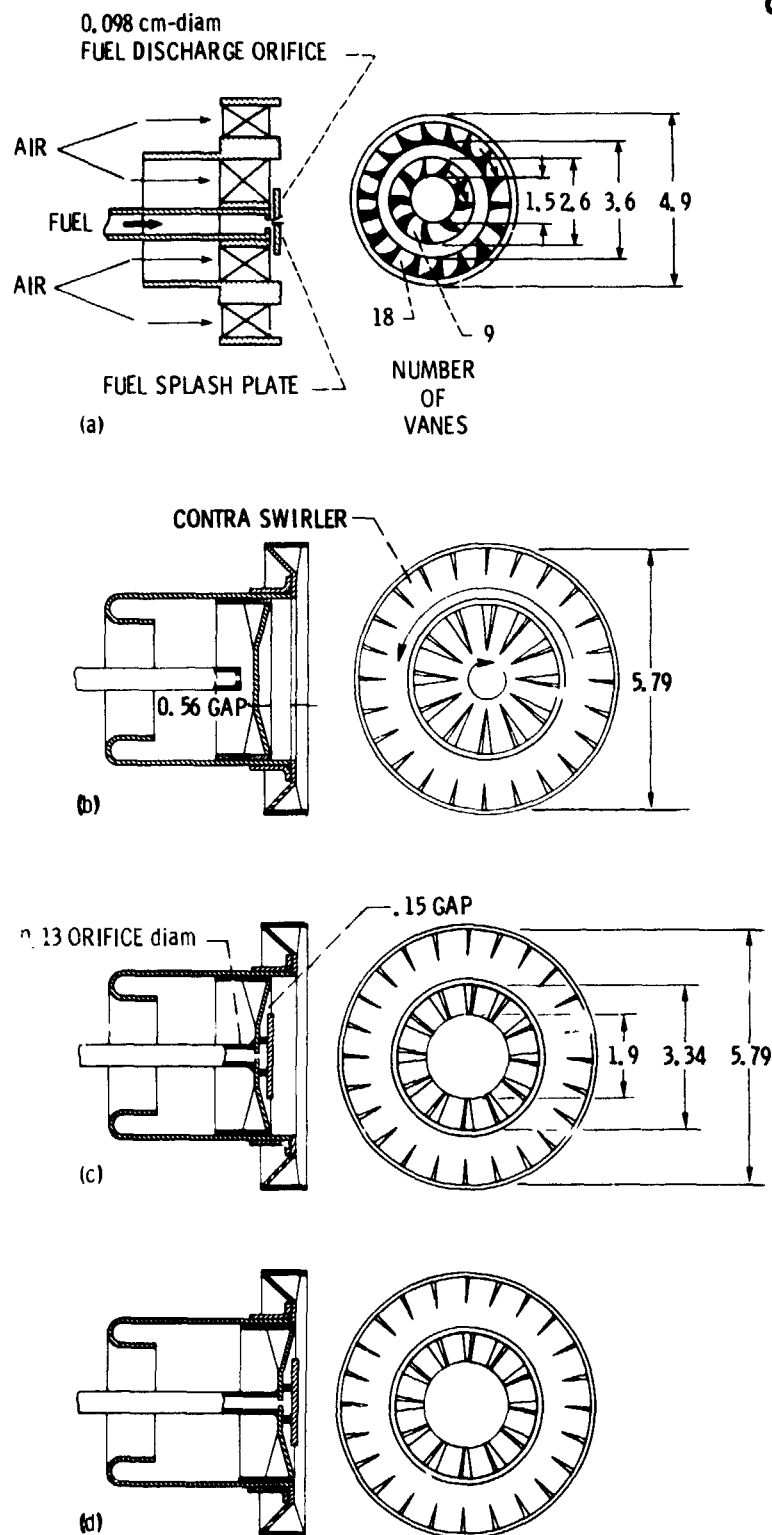




- (a) Splash-disk with single 0.1016 or 0.216 cm-diameter orifice.  
 (b) Splash-cone with four 0.157 cm-diameter orifices.  
 (c) Splash-groove with nine 0.051 cm-diameter orifices.

Figure 3. - Schematic diagram of splash-plate type fuel injectors.

ORIGINAL PAGE IS  
OF POOR QUALITY



- (a) Model used in reference 12 with fuel tubes having orifice diameters of 0.081 and 0.46 cm, respectively.
- (b) Model #8 (inner swirler recessed).
- (c) Model #9 (Injection downstream of swirler).
- (d) Model #10 (flush mounted swirlers).

Figure 4. - Swirl-can combustor modules (dimensions are in cm).

ORIGINAL PAGE IS  
OF POOR QUALITY

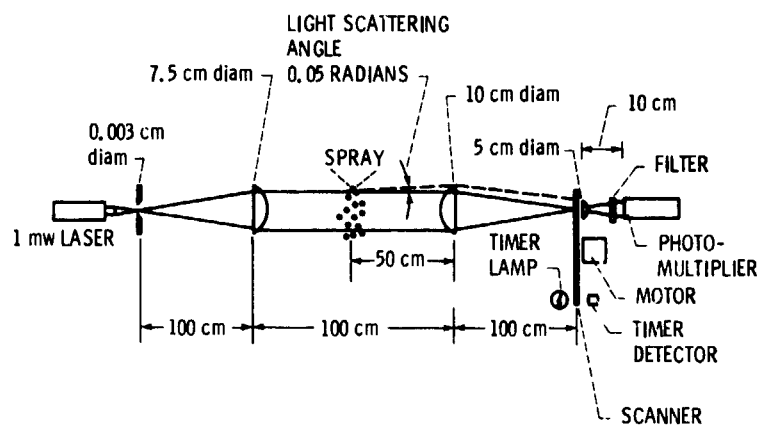


Figure 5. - Scanning radiometer optical path.

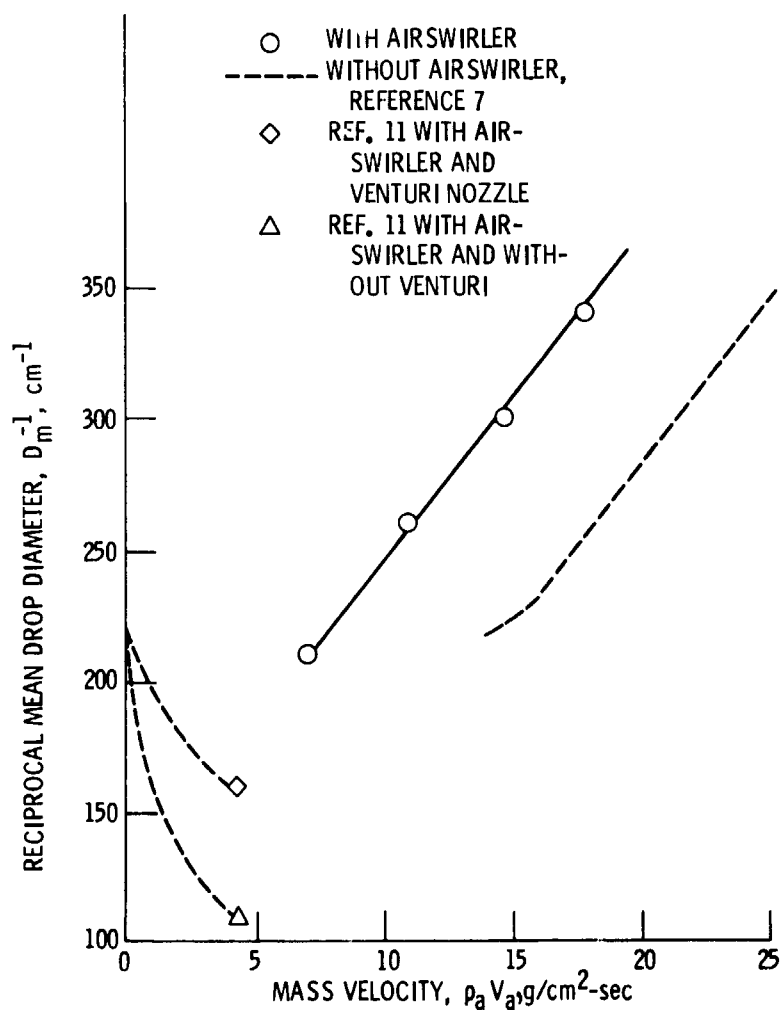


Figure 6. - Variation of reciprocal mean drop diameter with air-stream mass velocity for simplex pressure atomizing fuel nozzle #1, 0.090 cm-diam orifice and 45° cone angle.

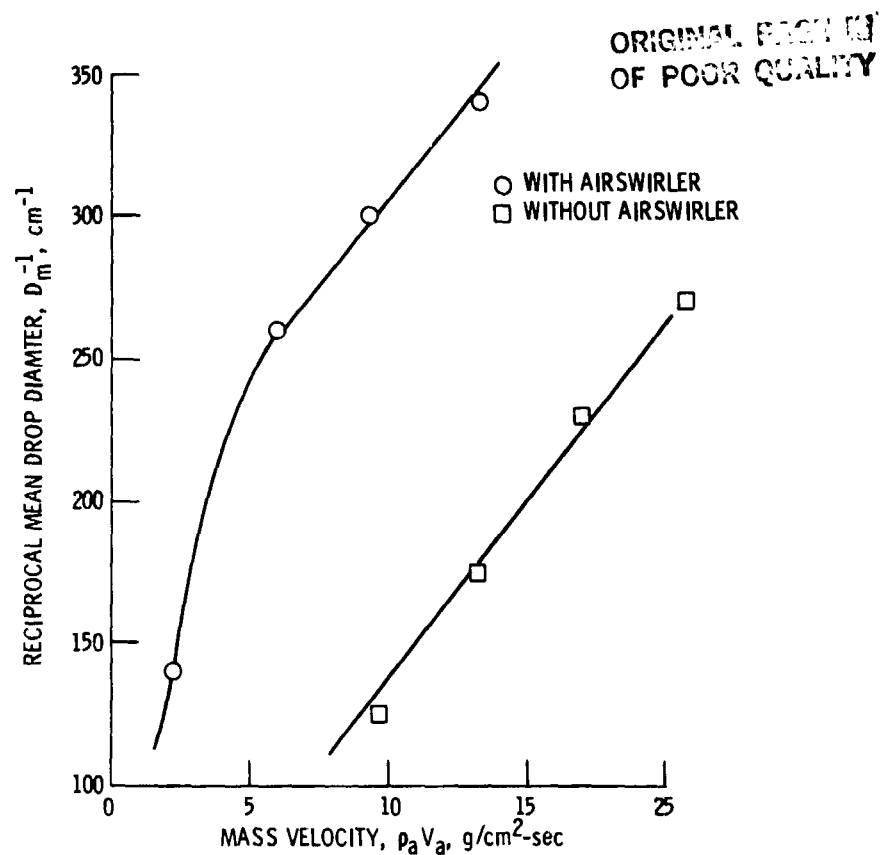


Figure 7. - Variation of reciprocal mean drop diameter with airstream mass velocity for simplex pressure atomizing fuel nozzle #2, 0.13 cm-diam orifice and 45° cone angle.

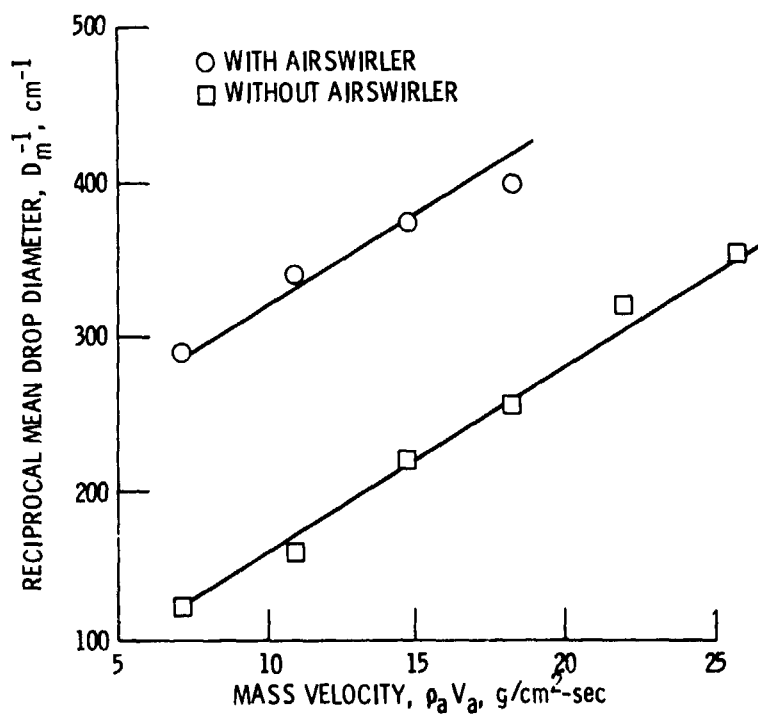


Figure 8. - Variation of reciprocal mean drop diameter with airstream mass velocity for simplex pressure atomizing fuel nozzle #3, 0.23 cm-diam orifice and 80° cone angle.

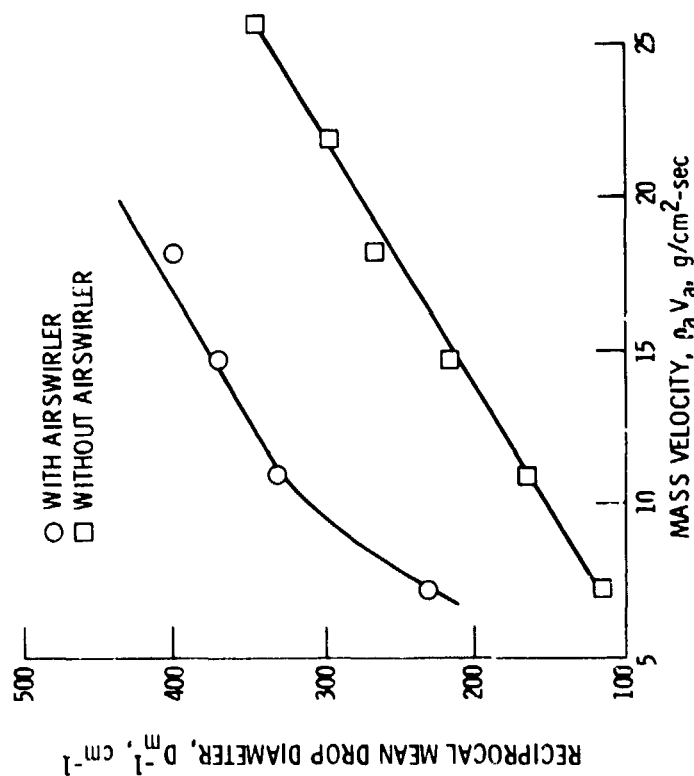


Figure 9. - Variation of reciprocal mean drop diameter with airstream mass velocity for simplex pressure atomizing fuel nozzle #4, 0.34 cm-diam orifice and 80° cone angle.

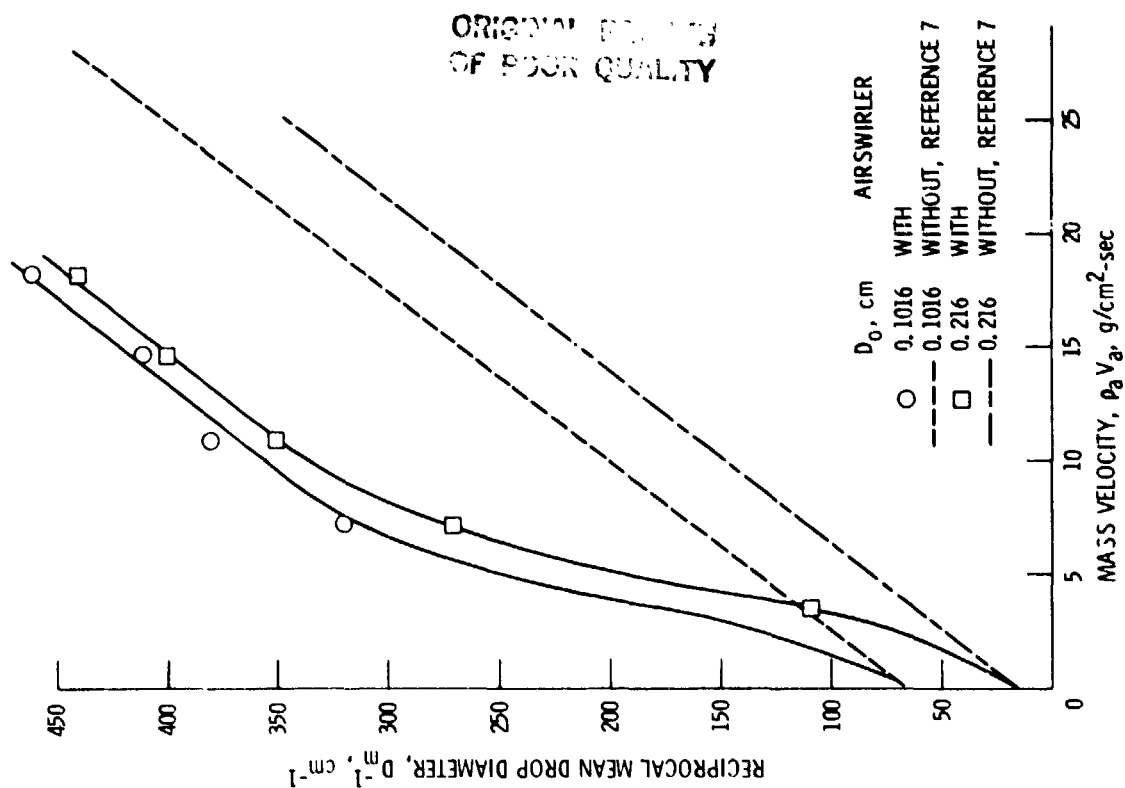


Figure 10. - Variation of reciprocal mean drop diameter with airstream mass velocity for splash disk fuel injectors.

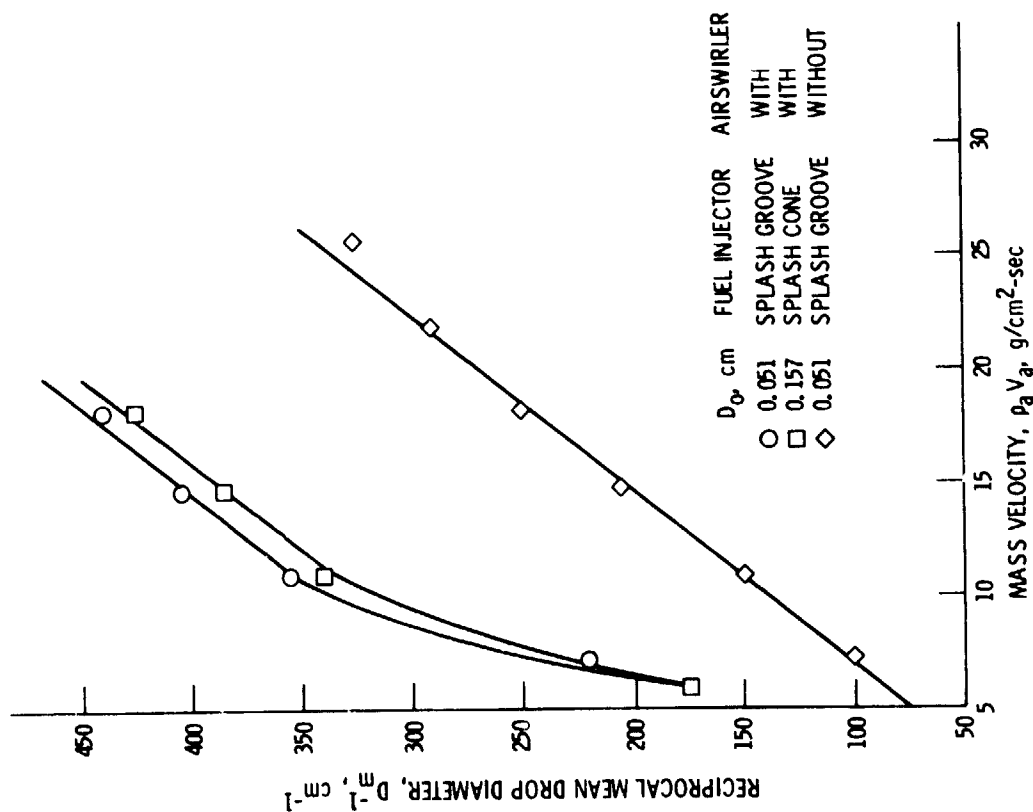


Figure 11. - Variation of reciprocal mean drop diameter with airstream mass velocity for splash groove and splash cone fuel injectors.

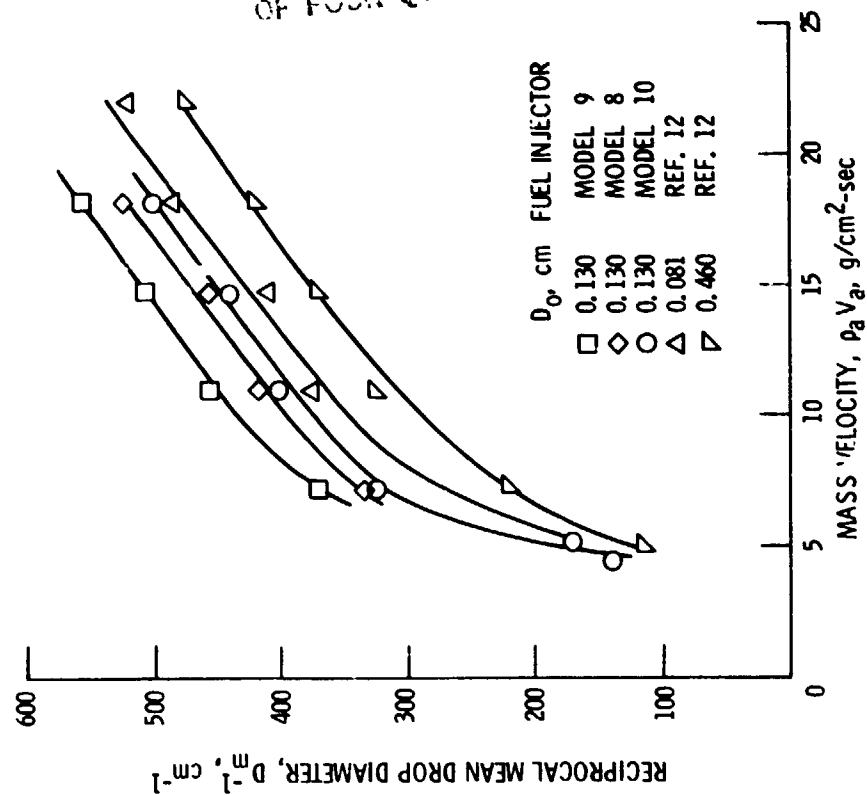


Figure 12. - Variation of reciprocal mean drop diameter with airstream mass velocity for swirl-can combustor modulus.

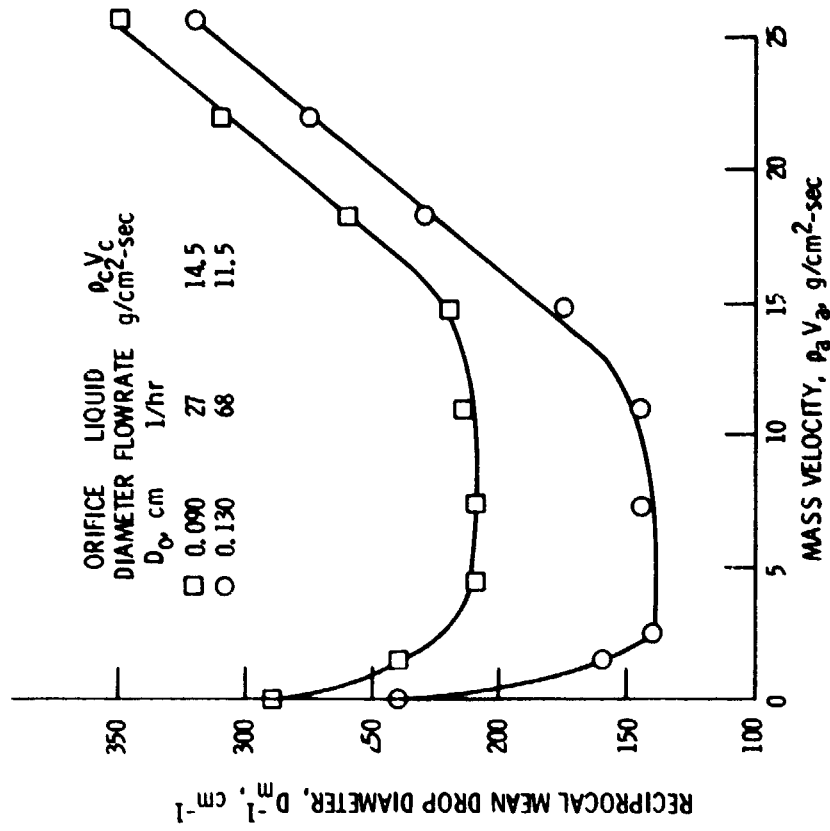


Figure 14. - Variation of reciprocal mean drop diameter,  $D_m^{-1}$ , with airstream mass velocity,  $\rho_a V_a$ , for simplex pressure atomizing nozzles, reference 7.

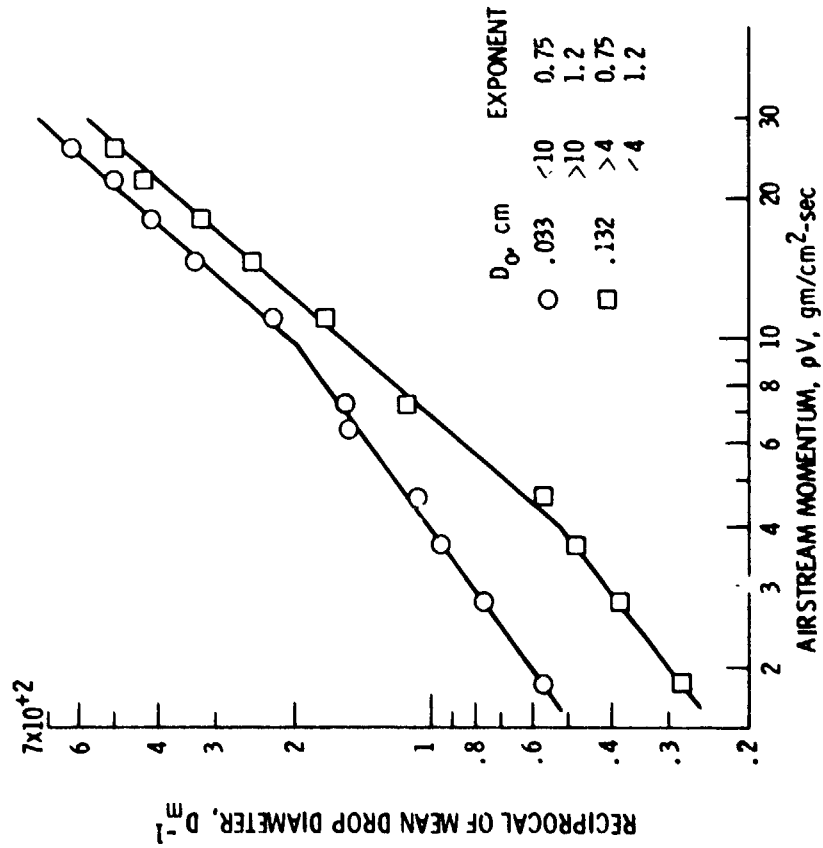


Figure 13. - Effect of airstream momentum on mean drop diameter,  $D_m^{-1}$ , reference 13.